CQE Center for Quantitative Economics

Metal Prices Made in China?
A Network Analysis of Industrial Metal Futures

Pierre L. Siklos [†] Martin Stefan [#] and Claudia Wellenreuther [#]

84/2019

[†] Department of Economics, Wilfrid Laurier University, Waterloo, Canada

[#] Department of Economics, University of Münster, Germany

wissen.leben
WWU Münster

Metal Prices Made in China? A Network Analysis of Industrial Metal Futures

Pierre L. Siklos [a] Martin Stefan [b]
Claudia Wellenreuther [c]

June 5, 2019

Abstract

Apart from being the world's greatest consumer and producer of industrial metals, China now also features the most actively traded industrial metal futures contracts worldwide. Using a sample of 29 futures contracts traded on exchanges in the United States, the United Kingdom, India and China, we estimate VAR models and conduct variance decompositions, which are then visualized in the form of networks. The results indicate that China is, despite its role as key actor in both real and financial industrial metal markets, a price taker.

Keywords: Commodity Markets, China, Industrial Metals, Price Leadership, Networks

[a]Department of Economics, Wilfrid Laurier University
[b]Department of Economics, Westfälische Wilhelms-Universität Münster
[c]Corresponding author: Department of Economics, Westfälische Wilhelms-Universität Münster, Am Stadtgraben 9, 48143 Münster, Germany, E-mail: Claudia.Wellenreuther@wiwi.uni-muenster.de

1 Introduction

China's rapid industrialization and rise as an economic power have been accompanied by a voracious appetite for natural resources. This is particularly visible in the country's demand for industrial metals. As the country continues its process of urbanization and investment in infrastructure, China has evolved into the world's top consumer of refined aluminum, copper, nickel, steel and zinc. In 1980, when the people's republic's policy of reform was just beginning, the country's share in the worldwide consumption of these metals ranged between three to four percent. Today, Chinese consumption makes up forty percent of the world's demand for lead and nickel and fifty percent of the world's demand for aluminum, copper and zinc (World Bank, 2018). Similarly, the country has also developed into the top producer of these metals. In 2017, roughly half of all steel, refined aluminium and zinc, and forty percent of refined copper and lead were produced in China (World Bank, 2018).

However, China's importance in the metal market is not limited to the real side of the economy. Chinese commodity futures exchanges have over the years, after a series of regulatory changes, evolved into the world's largest futures markets for numerous industrial metals. As documented by the Futures Industry Association's (FIA) 2017 volume survey, the seven most traded industrial metal futures contracts are traded on Chinese exchanges (Acworth 2017). Moreover, the Shanghai Futures Exchange's (SHFE) steel rebar futures contract has grown into the most traded commodity futures contract worldwide.

In light of these developments, this paper investigates the role of Chinese price leadership in industrial metals futures markets. We gather futures price data on 29 industrial metal contracts traded on six exchanges in the United States, the United Kingdom, India and China. To answer the question of whether China has become a price leader in these markets, the network approach of

Diebold & Yilmaz (2012, 2014) is used, which rests on variance decompositions of vector autoregressive (VAR) models' forecast errors. Based on these decompositions, so-called connectedness tables are compiled which summarize how shocks to a specific futures price travel through the system of all prices of this commodity. These connectedness tables are then visualized in the form of graphical networks.

We obtain two main findings. Chinese metal contracts are strongly interconnected with contracts traded on other exchanges. However, China is typically a net receiver of price shocks. This suggests that China is, despite its role as leading consumer, producer and trader of industrial metals, a price taker in the corresponding futures markets. The remainder of this paper is structured as follows. Section 2 summarizes important steps in the development of Chinese commodity futures markets and earlier research on their role as price leader. Thereafter, Section 3 explains the data used in this paper, while Section 4 introduces the methodology. Section 5 then presents the key results and Section 6 analyzes the determinants of connectedness. Lastly, Section 7 concludes.

2 Institutional background and related literature

Today, Chinese futures trading occurs on five futures exchanges. The Dalian Commodity Exchange (DCE) and the Zhengzhou Commodity Exchange (ZCE) mainly focus on agricultural and chemical products, while the Shanghai Futures Exchange (SHFE) covers various metal contracts. Financial and crude oil futures contracts are traded at the China Financial Futures Exchange (CFX) and the Shanghai International Energy Exchange (INE).

Despite the fact that Chinese futures markets continue to be relatively closed to foreign investors, who must generally rely on domestic intermediaries to

conduct trades on their behalf [1], many Chinese futures contracts now outstrip their Western counterparts in terms of trading volume. In international comparisons, Chinese metal futures contracts trade in remarkably high trading volumes, which is not surprising given the stylized facts outlined in the introduction. According to the FIA 2017 volume survey, the seven most traded industrial metal futures contracts are all traded on Chinese exchanges (Acworth 2017). Moreover, the Shanghai Futures Exchange (SHFE) steel rebar futures contract has grown into the most traded commodity futures contract in the world.

Against this backdrop, and given the fact that China has over the years evolved into the largest consumer and producer of numerous industrial metals (World Bank Group 2018), a sizable body of literature has investigated the role of Chinese futures exchanges as potential price leaders in industrial metals. Being among the oldest industrial metal futures contracts traded in China, the SHFE's copper contract has been analyzed in numerous studies. Fung et al. (2003) use data from 1995 to 2001 and conduct a bivariate GARCH analysis of two copper futures contracts traded at the SHFE and the New York Commodity Exchange (COMEX). They find that the American contract dominates the information flow between the two markets. Liu & An (2011) study the same contracts, but make use of a VECM-GARCH framework and a price discovery metric developed by Lien & Shrestha (2009). The authors use data from 2004 to 2009 and conclude that the U.S. market generally leads its Chinese counterpart and is also dominant in the price discovery process. Li & Zhang (2013) study the case of copper on a broader basis by considering, in addition to the contracts traded at the SHFE and the COMEX, also contracts traded at the London

[1] Exceptions pertain to the INE's crude oil contract, the DCE's iron ore contract and the ZCE's Purified Terephthalic Acid (PTA) contract, which, following a new directory by the China Securities Regulatory Commission (2015), can be traded directly by qualified foreign brokerage firms without the need for a domestic intermediary.

Metal Exchange (LME) and the Multi Commodity Exchange (MCX) in Mumbai, India. Employing an SVAR model and data ranging from 2005 to 2011, the authors' results suggest that the LME contract is the key price maker. Conversely, the results of Rutledge et al. (2013), who use a VECM estimation and Granger-causality tests based on data from 2006 to 2011, reveal no distinct leadership pattern between the copper contracts traded at the SHFE, the LME and the COMEX.

Studies featuring multiple metal contracts include that of Hua & Chen (2007), who study the markets for copper and aluminum. Using data from 1998 to 2002, the authors consider contracts traded at the SHFE and the LME. They employ Granger-causality tests and find that the LME contracts Granger-cause those of the SHFE, which implies that the Chinese contracts are price followers. Fung et al. (2010), who consider aluminum and copper contracts traded at the SHFE and the COMEX, use data from 1999 to 2009 and employ a VECM which accounts for structural breaks. They find that neither market dominates the information flow between them. Fung et al. (2013) investigate the case of Chinese price leadership on an even broader basis by considering 16 different commodities including aluminum, copper and zinc contracts traded at the SHFE and the LME. The authors' data range from different starting dates for each contract until 2011, and are analyzed using various regression techniques including error correction and GARCH models. Again, no clear pattern is found, as mixed and bidirectional results are obtained for the different industrial metal contracts. Lastly, the study by Kang & Yoon (2016), which is closely related to our work, uses the approach proposed by Diebold & Yilmaz (2012) to study the SHFE's and LME's futures contracts for aluminum, copper and zinc. Using data from 2007 to 2016, the authors find that price shocks typically originate in the LME's contracts and then travel to those of the SHFE.[2]

[2]Other applications of variance decompositions or the network approach of Diebold & Yilmaz

The present paper extends this earlier research in three important ways: First, by analyzing 29 different contracts, some of which were launched as recently as November 2015, it is the most comprehensive study of industrial metal futures conducted to date. As our analysis covers futures contracts for copper, lead, nickel, iron and several kinds of steel, we investigate a much larger variety of commodities than earlier studies. Second, by conducting variance-decompositions of the forecast errors of various systems of different futures contracts, the network approach of Diebold & Yilmaz (2012, 2014) enables us to graphically visualize the inter-dependencies between the different contracts. Third, we go beyond reporting market connectedness to consider the potential economic determinants of this phenomenon.

3 Data

To examine the role of Chinese price leadership in the market for industrial metal futures, we gather data on 29 industrial metal contracts at daily frequency. All price time series are retrieved from Thomson Reuters Datastream, whereby continuous series are constructed by switching to the nearest contract on the first day of each new trading month. Data availability dictates the span of the data set. Table 1 lists the contracts used in the analysis and details the different contract specifications such as notation and size.

[Table 1 about here.]

Our sample covers five aluminum contracts, one cobalt contract, four copper contracts, one ferrosilicon contract, two iron ore contracts, three lead and nickel contracts, one silicon manganese contracts, five steel contracts, one tin

(2012) to the case of Chinese commodity markets, include the studies of Yang & Leatham (1999) and Zhang & Wang (2014) who consider the markets for wheat and crude oil.

contract and three zinc contracts. The contracts are traded on six different exchanges, namely the New York Commodity Exchange (COMEX), the London Metal Exchange (LME), the Multi Commodity Exchange (MCX) (in Mumbai, India), the Shanghai Futures Exchange (SHFE), the Dalian Commodity Exchange (DCE) and the Zhengzhou Commodity Exchange (ZCE).

[Figure 1 about here.]

Figure 1 displays the futures prices time series of the commodity contracts included in our analysis. All prices have been converted to USD per metric ton (USD/mt). In accordance with the law of one price we observe relatively similar price movements among the different contracts for each type of commodity. Nonetheless, Chinese prices are most of the time noticeably higher for all commodities. This could be due to barriers to trade concerning the Chinese market. Regarding the steel market, we observe the greatest price differences within one commodity. This is because of the different types of steel included in our sample, ranging from steel rebar to steel coils and steel scrap. The same holds for the aluminum market, where one can see a large price difference between the LME's aluminum alloy contract and the other pure aluminum contracts. The unusual behaviour of the COMEX's aluminum price starting in late 2017 can be explained by the exceptionally low trading volumes of this contract.

[Table 2 about here.]

Summary statistics of the daily logarithmic futures returns are displayed in Table 2. The daily returns range from -0.32 percent to 0.33 percent. Standard deviations range from 0.01 to 0.03. Roughly two thirds of all return series exhibit a negative skewness, suggesting that severe price drops are more common than large price increases. For all return series we observe kurtosis values well in excess of 3, which is the reference kurtosis value of the normal distribution.

This implies that none of the series follow a normal distribution, but feature fat tails instead.

4 Methodology

To investigate the price leadership in the metal futures market, we follow the financial market connectedness approach of Diebold & Yilmaz (2012, 2014). This methodology suggests that the informational spillovers between different metal futures contracts are studied using a network interpretation of a vector autoregressive (VAR) model's variance decomposition. The starting point of this approach is estimating the following covariance stationary VAR(p) model:

$$\boldsymbol{r}_t = \sum_{i=1}^{p} \boldsymbol{\Phi}_i \, \boldsymbol{r}_{t-i} + \boldsymbol{\varepsilon}_t \, , \tag{1}$$

where the vector $\boldsymbol{r_t} = (r_{1,t},\ r_{2,t},\ \ldots,\ r_{n,t})'$ contains n logarithmic futures return time series and $\boldsymbol{\varepsilon}_t$ is a $n \times 1$ vector of white noise disturbances with covariance matrix $\boldsymbol{\Omega}$.

4.1 Forecast error variance decomposition

The VAR model above can be represented as a vector moving average (VMA) model of the form

$$\boldsymbol{r_t} = \sum_{i=0}^{\infty} \boldsymbol{\Psi_i} \, \boldsymbol{\varepsilon_{t-i}} \, , \tag{2}$$

where $\boldsymbol{\Psi_i}$ denote the $n \times n$ moving average coefficient matrices. These are determined by $\boldsymbol{\Psi_i} = \boldsymbol{\Phi}_1 \, \boldsymbol{\Psi}_{i-1} + \boldsymbol{\Phi}_2 \, \boldsymbol{\Psi}_{i-2} + \cdots + \boldsymbol{\Phi}_p \, \boldsymbol{\Psi}_{i-p}$ for $i > 0$, while $\boldsymbol{\Psi_0} = \boldsymbol{I}_n$ and $\boldsymbol{\Psi_i} = \boldsymbol{0}$ if $i < 0$. Based on the (VMA) model in equation (2), one can compute the generalized H-step ahead forecast error variance decompositions d_{ij}^{H}

of Koop et al. (1996) and Pesaran & Shin (1998) as

$$d_{ij}^{H} = \frac{\sigma_{jj}^{-1} \sum_{h=0}^{H-1} (\boldsymbol{e_i}' \boldsymbol{\Psi_h} \boldsymbol{\Omega} \boldsymbol{e_j})^2}{\sum_{h=0}^{H-1} (\boldsymbol{e_i}' \boldsymbol{\Psi_h} \boldsymbol{\Omega} \boldsymbol{\Phi_h}' \boldsymbol{e_i})} , \tag{3}$$

where σ_{jj} is the standard deviation of $\varepsilon_{j,t}$, while $\boldsymbol{e_i}$ is the $n \times 1$ selection vector consisting of zeros only except for its i-th element, which is equal to one. This decomposition captures the contribution that shocks to variable j make to the H-step-ahead error variance when forecasting variable i. In the case of $i = j$, Diebold & Yilmaz (2012) refer to this as *own variance share*. Correspondingly, if $i \neq j$, d_{ij}^{H} is called *cross variance share*.

Note that this type of variance decomposition, unlike conventional variance decompositions, does not make use of a Cholesky factorization of $\boldsymbol{\Omega}$ and is thus independent from the ordering of the time series in the system. However, as the shocks to the model's variables are not orthogonalized, a variable i's different variance shares due to shocks in variables j generally do not add up to one, i.e. $\sum_{j=1}^{n} d_{ij}^{H} \neq 1$. Therefore, and to allow straightforward comparisons between the different shocks sent by a variable j to other variables i, the variance decompositions are normalized and converted into percentages by computing

$$\tilde{d}_{ij}^{H} = \frac{d_{ij}^{H}}{\sum_{j=1}^{n} d_{ij}^{H}} \cdot 100 . \tag{4}$$

Thus, it holds by construction that $\sum_{j=1}^{n} \tilde{d}_{ij} = 100$ and that $\sum_{i,j=1}^{n} \tilde{d}_{ij} = n \cdot 100$.[3]

[3] An alternative forecast error variance decomposition is developed by Lanne & Nyberg (2016).

4.2 Measuring connectedness

Following Diebold & Yilmaz (2014), the variance decomposition computed above can be interpreted as a measure for the H-step ahead *gross* pairwise directional connectedness from variable j to variable i, i.e.

$$C^H_{i \leftarrow j} = \tilde{d}^H_{ij} \ . \tag{5}$$

As $C^H_{i \leftarrow j}$ will generally not be equal to $C^H_{j \leftarrow i}$, the net flow of shocks between the two variables, or *net* pairwise directional connectedness from variable j to variable i, is calculated as

$$C^H_{ij} = \tilde{d}^H_{ji} - \tilde{d}^H_{ij} \ . \tag{6}$$

To gauge a variable's relative importance as sender or receiver of shocks in the system, Diebold & Yilmaz (2014) compute two measures of *total* directional connectedness. The first of these measures, $C^H_{i \leftarrow \bullet}$, summarizes all those parts of a variable i's forecast error variance decomposition that are due to shocks *from* other variables j. Hence, this measure is calculated as

$$C^H_{i \leftarrow \bullet} = \sum_{\substack{j=1, \\ j \neq i}}^{n} \tilde{d}^H_{ij} \ . \tag{7}$$

Conversely, the second measure $C^H_{\bullet \leftarrow j}$ summarizes all the contributions that variable i makes *to* the forecast error variance decompositions of other variables j. This measure is therefore given by

$$C^H_{\bullet \leftarrow j} = \sum_{\substack{i=1, \\ i \neq j}}^{n} \tilde{d}^H_{ij} \ . \tag{8}$$

Lastly, to capture the system's total connectedness, Diebold & Yilmaz (2014) sum up all of the normalized cross variance shares. To allow comparing the

total connectedness values of different variable systems, this measure C^H is also normalized by n:

$$C^H = \frac{1}{n} \sum_{\substack{i,j=1, \\ i \neq j}}^{n} \tilde{d}_{ij}^H \, . \tag{9}$$

It holds by construction that the system's total connectedness is equal to the (normalized) sum of all shocks sent or equivalently all shocks received.

Given these measures of connectedness, a *connectedness table* for the VAR system of equation (1) is constructed as follows:

[Table 3 about here.]

The main diagonal elements, apart from C^H, display how the variance of a specific return series is driven by the series's own shocks. The off-diagonal elements, except those at the margin of the connectedness table, represent the fraction of a return series's variance that is due to shocks in the other return series. The bottom row elements summarize the total impact that the return series have on the variance of the other return series, while the elements of the rightmost column summarize the total of shocks that the return series receive from the other series in the system. Thus, the greater a futures return series's total directional connectedness is, the greater its role in price leadership. Conversely, if a return series features a large row sum, it features a high total directional connectedness from others and is therefore a strong recipient of price signals originating from other futures contracts.

As suggested by Diebold & Yilmaz (2014) the $n \times n$ variance decompositions matrix is essentially a network adjacency matrix. The nodes of this network are the different variables of the VAR system, i.e. in our case the different metal futures contracts, while the connections between the contracts are determined by the magnitudes of the different variance decompositions. The advantage of interpreting the variance decompositions in this way, is that it allows

straightforward visualizations of market inter-dependencies and information flows, which are discussed below in greater detail.

5 Results of the network analysis

As the first part of the analysis, we consider the entire sample of industrial metal futures contracts explained in the data section. The resulting system comprises 29 contracts across eleven different commodities traded on six futures exchanges in four countries. The sample size is thereby limited by the contracts with the most recent starting dates. These are the SHFE's steel contracts, which started trading in November 2015. The sample ends in October 2018. We implement the variance decomposition procedure described above and, following Diebold & Yilmaz (2014), we interpret the resulting connectedness table as a network. As explained before, each node in the network resembles one of the futures contracts.

Figure 2 visualizes this network based on the graph drawing algorithm developed by Fruchterman & Reingold (1991). This algorithm draws networks by balancing attracting and repelling forces between its nodes. In our network two nodes attract each other depending on their pairwise directional spillovers. The net pairwise directional spillovers, i.e. the differences between the two shocks flowing between two contracts, are shown as arrows between the nodes. They point in the direction of the larger shock between the two contracts and are the thicker the greater the net directional spillover. The nodes repel each other depending on their size which is determined by the total directional connectedness *to* others. Consequently, strong net senders of shocks will feature large nodes with numerous arrows pointing away from them. Conversely, strong recipients have smaller nodes and many arrows pointing toward them. Lastly, the nodes are highlighted in different colors depending on the contracts' un-

derlying commodities.

[Figure 2 about here.]

The network visualization reveals distinct clusters of contracts based on the underlying commodity groups to which they belong. Copper contracts are located close to other copper contracts, aluminum contracts close to other aluminum contracts and so on. Only the steel contracts (highlighted in orange) are relatively spread out, but they still form a cluster. The steel cluster partly surrounds the iron cluster (highlighted in cyan) reflecting the close relationship between the two commodities. The center of the network is dominated by the different copper contracts (highlighted in red). Apart from their placement in the center of the network, the nodes of these contracts are also considerably larger than those of other commodity groups underscoring their importance for the network. This is in line with the fact that copper is one of the most widely used industrial metals featuring applications in construction, electrical and electronic products, transportation and consumer products. Therefore, copper is by some commentators seen as an indicator for the state of the overall economy.

The nickel and zinc clusters (highlighted in green and yellow, respectively) also feature relatively large nodes that are also placed toward the center of the network. This mirrors their great importance in the real metal market, where nickel and zinc are highly connected to other metals as they are used for the galvanization and production of stainless steel and other ferro-alloys. The aluminum and lead clusters (highlighted in blue and gray, respectively) tend toward the periphery of the network but are not as distant from the center as the contracts for cobalt, ferrosilicon, silicon manganese and tin. In the network, lead is closely connected to zinc, reflecting the fact that lead is a common byproduct in the zinc mining process.

Concerning the Chinese futures contracts, we find that these contracts are, despite their large trading volumes, generally of minor importance to the network as indicated by their relatively small node sizes and the high number of arrows pointing toward them.

In a second step, we now consider the financial connectedness within the different clusters of commodities observed above. In this regard, we examine six clusters, namely those of aluminum, copper, lead, nickel, zinc and the combined cluster of iron and steel. As before, the sample sizes are limited by the youngest contract in each cluster.[4] The resulting subnetworks are shown in figure 3. The subnetworks confirm the earlier impression that the Chinese contracts are price takers. In all of the six clusters, the Chinese contracts feature the smallest nodes. Despite their placement often in the center of the networks, they are major recipients of shocks from the others markets, as shown by the net pairwise directional spillovers pointing toward them.

[Figure 3 about here.]

To study the subnetworks over time, we employ rolling window estimations of the underlying VAR models with a window size of 250 trading days, which is equal to one trading year. In each step, we follow the variance decomposition procedure as before. Thereafter, we move the window ahead by one day for the subsequent estimation. Consequently, we obtain for each day and futures contract the total directional spillovers *to others* and *from others*. While the former measure the amount of shocks sent by the different markets, the latter capture the amount of shocks received by each of them. Computing the differences between these two metrics yields the *net* total directional spillovers. If a market's net spillover is above zero, the market sends more shocks than

[4]The aluminum sample starts on 6 May 2014, the copper sample on 18 November 2004, the lead sample on 24 March 2011, the nickel sample on 27 March 2015, the iron and steel sample on 23 November 2015, and the zinc sample on 26 March 2007. All samples end on 12 October 2018.

it receives. Conversely, if the market's net spillover is below zero, the market is a net-receiver of price signals. Figure 4 displays these time-varying *net* total directional spillovers of each futures contract.

[Figure 4 about here.]

The graphs show that for most of the commodity clusters the net spillovers range between -60 and 30. However, the steel market exhibits far smaller net spillovers ranging from only -20 to 10. This suggests that the iron and steel market is less integrated than the other commodity groups, which is not surprising given the different types of underlyings of these contracts (rebar, coils etc.). This corresponds to what has been found in figure 2, where the steel and iron contracts were relatively spread out. The net spillovers of Chinese contracts are almost always below zero and relatively stable over time, which supports our initial finding that the Chinese exchanges are net-receivers of shocks.

6 Determinants of connectedness

In this section we analyze which factors determine if a market is a sender or a receiver of price signals. Therefore, we regress the pairwise directional spillovers $C^{10}_{i\leftarrow j, i\neq j}$ between contracts j and i on several exogenous variables. In particular we estimate for each of the commodity subnetworks the following dynamic panel fixed effects regression:

$$\begin{aligned} C^{10}_{i\leftarrow j,t} = \; & \beta_0 + \beta_1 C^{10}_{i\leftarrow j,t-1} + \beta_2 VOLA_{j,t} + \beta_3 ILLIQ_{j,t} + \\ & \beta_4 SPMAT_{j,t} + \beta_5 IM_{ij,t} + \beta_6 EX_{ij,t} + \\ & \beta_7 TED_{j,t} + \beta_8 VIX_{j,t} + \beta_9 EPU_{j,t} + \varepsilon_{j,t} \, . \end{aligned} \tag{10}$$

Apart from the lagged spillover variable $C^{10}_{i\leftarrow j,t-1}$, we consider three groups

of exogenous variables, namely financial variables, variables related to real economic activity and variables measuring credit risk and market uncertainty. The financial group includes the variables $VOLA_{j,t}$ and $ILLIQ_{j,t}$. $VOLA_{j,t}$ refers to the relative market volatility of contract j, which is based on the conditional volatility estimates of an AR(1)-GARCH(1,1) model of contract j's returns. $ILLIQ_{j,t}$ is a proxy for market illiquidity proposed by Amihud (2002), which relates the absolute value of a market's return to its trading volume. High values of this ratio indicate illiquid market environments, whereas low values of this measure suggest high levels of liquidity. It is generally expected that liquidity increases a market's ability to process new information.

The second group of variables, which capture economic activity, comprise the regressors $SPMAT_{j,t}$, $IM_{ij,t}$, and $EX_{ij,t}$. To control for regional supply and demand shocks, we consider the S&P 500 Materials $SPMAT_{j,t}$ for the US, Europe, India and China. $IM_{ij,t}$ and $EX_{ij,t}$ refer to the imports and exports flowing between country i and country j, whereby $IM_{ij,t}$ represents the amount of the underlying commodity that country j imports from i, while $EX_{ij,t}$ denotes exports from j to i. Another important economic variable is the exchange rate. We consider the dollar exchange rate of the currency the contract is denominated in. If a contract is denominated in dollar, which is the case for contracts traded at the COMEX and the LME, we use the inverse of the trade-weighted US dollar index, called the broad index.

However, given the interdependencies between exports, imports and the exchange rate and the resulting endogeneity problem, we do not consider the exchange rate in the main regression. Instead we follow an instrumental variables approach using a two-stage least square estimation. In the first stage we regress imports and exports on the lagged values of imports, exports and the exchange rate. The fitted values of this first stage regressions are then used to estimate equation (10).

The third group comprises the variables $TED_{j,t}$, $VIX_{j,t}$ and $EPU_{j,t}$. The TED-spread $TED_{j,t}$ is a measure for credit risk and is calculated as the difference between the benchmark interbank lending rates and the interest rates of the corresponding government securities. The volatility index $VIX_{j,t}$ captures the volatility of the countries' major stock exchange indices and is a common proxy for market uncertainty. The variable $EPU_{j,t}$ is an index measuring the economic policy uncertainty of the country in which contract j is traded. Lastly, β_0 denotes a constant and $\varepsilon_{j,t}$ the error term.

We obtain data from three sources. Price and volume data are taken from Thomson Reuters Datastream to compute $VOLA_{j,t}$ and $ILLIQ_{j,t}$. Similarly, interest rate data for the $TED_{j,t}$ as well as the $VIX_{j,t}$, and data for the $SPMAT_{j,t}$ and the exchange rates are all retrieved from Thomson Reuters Datastream. Lastly, the economic policy uncertainty indices $EPU_{j,t}$ are developed by Baker et al. (2016)[5], while $IM_{ij,t}$ and $EX_{ij,t}$ are obtained from the International Trade Centre (ITC).

[Table 4 about here.]

The results of the regressions are presented in table 4. The lagged spillovers are significantly positive in all subnetworks. The relative volatility has a significantly negative impact for copper, lead and zinc. This indicates that contracts with higher volatility send less information to other contracts than contracts with lower levels of volatility. The Amihud-ratio, which captures market illiquidity, is associated with a significantly negative sign in the lead market, which implies that liquidity improves this market's ability to transmit information. Concerning the other real economy variables, we find that imports are never significant. Exports, however, show a significantly positive influence in the

[5]Data for the economic policy uncertainty indices by Baker et al. (2016) are available at www.PolicyUncertainty.com.

copper and zinc markets. The impact of the S&P 500 Materials index is significantly positive in the iron and steel network. The results regarding the VIX indices are inconclusive as coefficients with differing signs are obtained for the different subnetworks. The EPU indices exhibit a significantly positive influence in the copper and iron and steel networks, while the TED-spread is only significantly positive in the zinc network.

7 Conclusion

In the past two decades, China has become the greatest consumer and producer of numerous industrial metals. Moreover, China has recently launched a number of futures contracts for these metals and these have become some of the most traded futures contracts worldwide. This paper investigates the question of whether these new markets are important in the formation of international prices. We follow the network approach by Diebold & Yilmaz (2012, 2014) and consider 29 metal contracts, traded on six exchanges in the United States, the United Kingdom, India and China. However, despite their large trading volumes, our results indicate that these Chinese futures contracts are not price leaders.

Our analysis comprised three steps. First, we analyzed the overall network structure across all industrial metal futures contracts included in our sample. Unsurprisingly, futures contracts of the same underlying commodities were grouped closely together. Of these clusters, the copper and zinc clusters were found to be the most important ones regarding the transmission of price signals. Furthermore, the Chinese contracts appeared to play a minor role within the different commodity clusters. In the second step, we repeated the earlier analysis, but for each of the different commodity clusters separately. The results of this step confirmed those of the first one: Chinese contracts were again found

to be net-recipients of price shocks. Next, we conducted time-varying network analyses to study how China's role of price leadership varies over time. The results implied that China's passive role in the price discovery process is relatively stable over time. Lastly, we used a dynamic fixed effects panel regression to study the determinants of connectedness. Apart from lagged spillovers, relative volatility seemed to be the strongest determinant of connectedness.

In conclusion, our results provide strong evidence that metal prices are currently not made in China. Over the past years, Chinese regulators have been able to develop active futures markets for many different commodities including various industrial metals. However, further steps have to be taken to strengthen the role of Chinese markets in terms of price leadership. Most importantly, Chinese markets must become more accessible to foreign investors. A first step in this direction might be the opening of the DEC iron ore futures contract to overseas investors in May 2018. It remains to been seen whether such action will strengthen the international position of Chinese futures contracts.

References

Acworth, W. (2017), 'Annual volume survey', *Market Voice* .

Amihud, Y. (2002), 'Illiquidity and stock returns: cross-section and time-series effects', *Journal of Financial Markets* **5**(1), 31–56.

Baker, S. R., Bloom, N. & Davis, S. J. (2016), 'Measuring economic policy uncertainty', *The Quarterly Journal of Economics* **131**(4), 1593–1636.

China Securities Regulatory Commission (2015), 'Interim measures for overseas traders and overseas brokers to manage futures of certain types of futures', (See: http://www.dce.com.cn/dalianshangpin/fg/fz/jysgzhgz/2048658/index.html).

Diebold, F. X. & Yilmaz, K. (2012), 'Better to give than to receive: Predictive directional measurement of volatility spillovers', *International Journal of Forecasting* **28**(1), 57–66.

Diebold, F. X. & Yilmaz, K. (2014), 'On the network topology of variance decompositions: Measuring the connectedness of financial firms', *Journal of Econometrics* **182**(1), 119–134.

Fruchterman, T. M. J. & Reingold, E. M. (1991), 'Graph drawing by force-directed placement', *Software: Practice and Experience* **21**(11), 1129–1164.

Fung, H.-G., Leung, W. K. & Xu, X. E. (2003), 'Information flows between the U.S. and China commodity futures trading', *Review of Quantitative Finance and Accounting* **21**(3), 267–285.

Fung, H.-G., Liu, Q. W. & Tse, Y. (2010), 'The information flow and market efficiency between the U.S. and Chinese aluminum and copper futures markets', *Journal of Futures Markets* **30**(12), 1192–1209.

Fung, H.-G., Tse, Y., Yau, J. & Zhao, L. (2013), 'A leader of the world commodity futures markets in the making? the case of China's commodity futures', *International Review of Financial Analysis* **27**, 103–114.

Hua, R. & Chen, B. (2007), 'International linkages of the Chinese futures markets', *Applied Financial Economics* **17**(16), 1275–1287.

Kang, S. H. & Yoon, S.-M. (2016), 'Dynamic spillovers between Shanghai and London nonferrous metal futures markets', *Finance Research Letters* **19**, 181–188.

Koop, G., Pesaran, M. & Potter, S. M. (1996), 'Impulse response analysis in nonlinear multivariate models', *Journal of Econometrics* **74**(1), 119–147.

Lanne, M. & Nyberg, H. (2016), 'Generalized forecast error variance decomposition for linear and nonlinear multivariate models', *Oxford Bulletin of Economics and Statistics* **78**(4), 595–603.

Li, Z. & Zhang, L. H. (2013), 'An empirical study of international linkages of the Shanghai copper futures market', *The Chinese Economy* **46**(3), 61–74.

Lien, D. & Shrestha, K. (2009), 'A new information share measure', *Journal of Futures Markets* **29**(4), 377–395.

Liu, Q. & An, Y. (2011), 'Information transmission in informationally linked markets: Evidence from US and Chinese commodity futures markets', *Journal of International Money and Finance* **30**(5), 778–795.

Pesaran, H. H. & Shin, Y. (1998), 'Generalized impulse response analysis in linear multivariate models', *Economics Letters* **58**(1), 17–29.

Rutledge, R. W., Karim, K. & Wang, R. (2013), 'International copper futures market price linkage and information transmission: Empirical evidence from

the primary world copper markets', *Journal of International Business Research* **12**(1).

World Bank Group (2018), 'Commodity markets outlook, April 2018', *World Bank, Washington, DC* .

Yang, J. & Leatham, D. J. (1999), 'Price discovery in wheat futures markets', *Journal of Agricultural and Applied Economics* **31**(2), 359–370.

Zhang, B. & Wang, P. (2014), 'Return and volatility spillovers between China and world oil markets', *Economic Modelling* **42**, 413–420.

Table 1: Industrial Metal Futures Contracts

Contract	Exchange	Notation	Size
Aluminum	COMEX	USD/mt	25 mt
Aluminum	LME	USD/mt	25 mt
Aluminum Alloy	LME	USD/mt	20 mt
Aluminum	MCX	INR/kg	5 mt
Aluminum	SHFE	RMB/mt	5 mt
Cobalt	LME	USD/mt	1 mt
Copper	COMEX	USD/lbs	25000 lb
Copper	LME	USD/mt	25 mt
Copper	MCX	INR/kg	1 mt
Copper	SHFE	RMB/mt	5 mt
Ferrosilicon	ZCE	RMB/mt	5 mt
Iron Ore	DCE	RMB/mt	100 mt
Iron Ore	COMEX	USD/mt	500 mt
Lead	LME	USD/mt	25 mt
Lead	MCX	INR/kg	5 mt
Lead	SHFE	RMB/mt	5 mt
Nickel	LME	USD/mt	6 mt
Nickel	MCX	INR/kg	250 kg
Nickel	SHFE	RMB/mt	1 mt
Silicon Manganese	ZCE	RMB/mt	5 mt
Steel Scrap	LME	USD/mt	10 mt
Steel Rebar	LME	USD/mt	10 mt
Steel Coils	COMEX	USD/st	20 st
Steel Rebar	SHFE	RMB/mt	10 mt
Steel Coils	SHFE	RMB/mt	10 mt
Tin	LME	USD/mt	5 mt
Zinc	LME	USD/mt	25 mt
Zinc	MCX	INR/kg	5 mt
Zinc	SHFE	RMB/mt	5 mt

Note: The exchange abbreviations "COMEX", "LME", "MCX", "SHFE", "DCE" and "ZCE" refer to the New York Commodity Exchange, the London Metal Exchange, the Multi Commodity Exchange (Mumbai, India), the Shanghai Futures Exchange, the Dalian Commodity Exchange and the Zhengzhou Commodity Exchange. The currency abbreviations "USD", "RMB" and "INR" refer to the U.S. dollar, the Chinese renminbi and the Indian rupee. Contract sizes are reported in "mt","kg" and "st","lb" referring to metric tons and kilograms, and short tons (equivalent to roughly 0.907 metric tons) and pounds (equivalent to 0.453 kilograms).

Table 2: Summary Statistics of Returns

Contract	Exchange	Min	Mean	Max	St.dev.	Skew.	Kurt.
Aluminum	COMEX	-0.04	0.00	0.04	0.01	0.06	4.74
Aluminum	LME	-0.08	0.00	0.05	0.01	0.18	5.93
Aluminum Alloy	LME	-0.07	-0.00	0.06	0.01	-0.17	11.23
Aluminum	MCX	-0.10	0.00	0.07	0.01	0.15	10.00
Aluminum	SHFE	-0.04	-0.00	0.04	0.01	0.18	5.54
Cobalt	LME	-0.13	0.00	0.12	0.02	0.19	19.86
Copper	COMEX	-0.12	0.00	0.12	0.02	-0.13	7.06
Copper	LME	-0.10	0.00	0.12	0.02	-0.01	7.30
Copper	MCX	-0.12	0.00	0.10	0.02	-0.16	7.35
Copper	SHFE	-0.07	0.00	0.06	0.01	-0.28	6.07
Ferrosilicon	ZCE	-0.28	0.00	0.20	0.02	-2.86	53.71
Iron Ore	DCE	-0.32	-0.00	0.10	0.03	-3.18	35.00
Iron Ore	COMEX	-0.09	-0.00	0.16	0.02	0.28	7.46
Lead	LME	-0.08	-0.00	0.08	0.02	-0.01	5.27
Lead	MCX	-0.09	-0.00	0.08	0.01	-0.04	5.64
Lead	SHFE	-0.05	-0.00	0.05	0.01	-0.15	7.53
Nickel	LME	-0.09	-0.00	0.07	0.02	-0.23	4.43
Nickel	MCX	-0.08	-0.00	0.07	0.02	-0.02	4.42
Nickel	SHFE	-0.06	-0.00	0.06	0.01	-0.10	5.21
Silicon Manganese	ZCE	-0.28	0.00	0.33	0.03	0.49	65.58
Steel Scrap	LME	-0.08	0.00	0.10	0.02	-0.29	7.21
Steel Rebar	LME	-0.04	0.00	0.05	0.01	0.19	6.04
Steel Coils	COMEX	-0.06	0.00	0.11	0.01	1.81	20.48
Steel Rebar	SHFE	-0.09	0.00	0.08	0.02	-0.24	6.15
Steel Coils	SHFE	-0.08	0.00	0.08	0.02	0.02	7.20
Tin	LME	-0.04	0.00	0.04	0.01	-0.10	4.59
Zinc	LME	-0.11	-0.00	0.10	0.02	-0.06	5.40
Zinc	MCX	-0.09	-0.00	0.10	0.02	-0.12	5.50
Zinc	SHFE	-0.06	-0.00	0.05	0.01	-0.40	5.64

Note: The exchange abbreviations "COMEX", "LME", "MCX", "SHFE", "DCE" and "ZCE" refer to the New York Commodity Exchange, the London Metal Exchange, the Multi Commodity Exchange (Mumbai, India), the Shanghai Futures Exchange, the Dalian Commodity Exchange and the Zhengzhou Commodity Exchange.

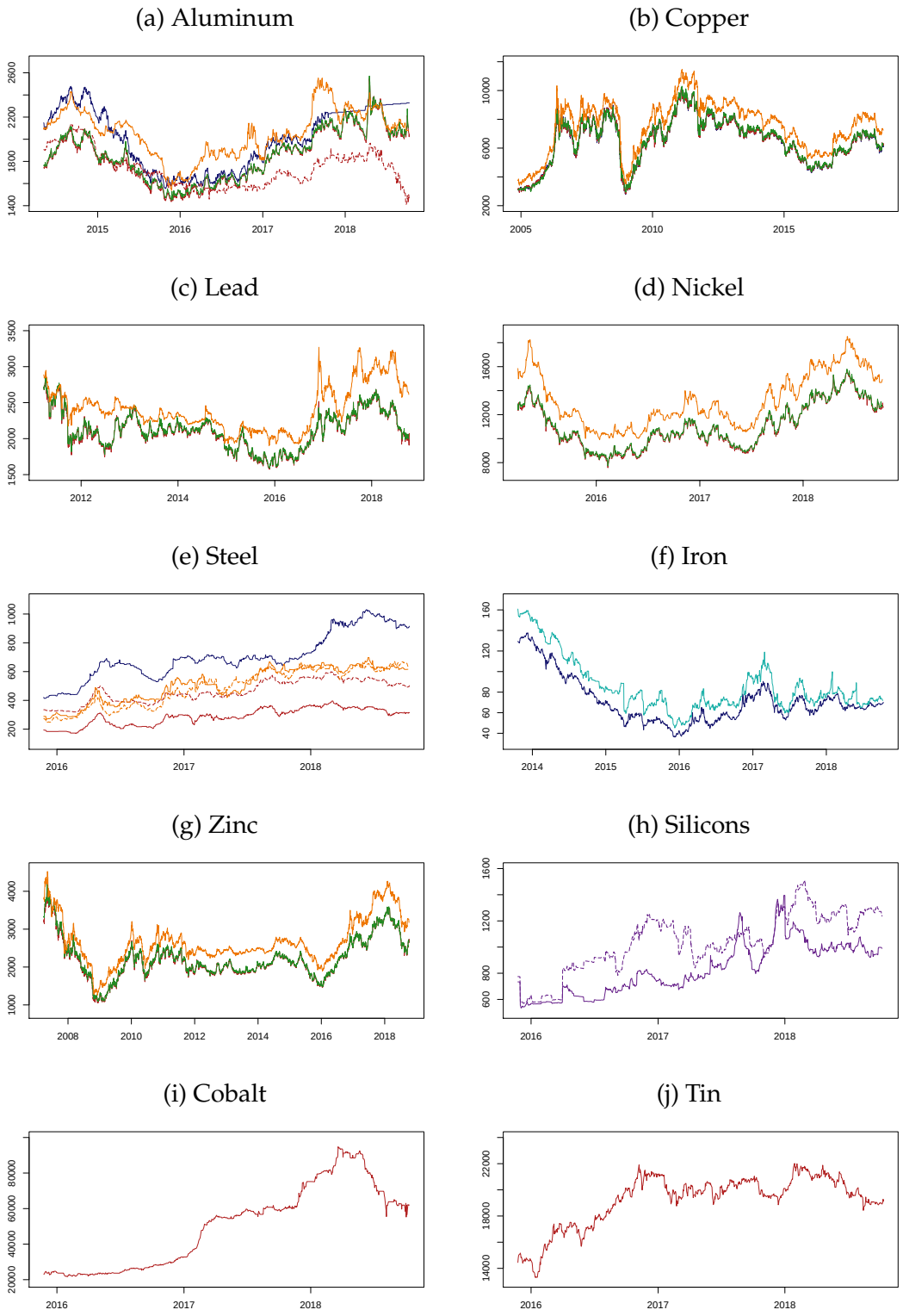

Figure 1: Futures Price Time Series

Note: COMEX contracts are highlighted in blue, LME contracts in red, MCX contracts in green, SHFE contracts in orange, DCE contracts in cyan, ZCE contracts in purple. Steel rebar, aluminum alloy and the silicon manganese contracts are depicted using dashed lines. All prices have been converted to USD/mt.

Table 3: Concept of Connectedness Tables

	r_1	r_2	$\dots$	r_n	From others
r_1	$C^H_{1\leftarrow 1}$	$C^H_{1\leftarrow 2}$	$\dots$	$C^H_{1\leftarrow n}$	$C^H_{1\leftarrow \bullet}$
r_2	$C^H_{2\leftarrow 1}$	$C^H_{2\leftarrow 2}$	$\dots$	$C^H_{2\leftarrow n}$	$C^H_{2\leftarrow \bullet}$
$\vdots$	$\vdots$	$\vdots$	$\ddots$	$\vdots$	$\vdots$
r_n	$C^H_{n\leftarrow 1}$	$C^H_{n\leftarrow 2}$	$\dots$	$C^H_{n\leftarrow n}$	$C^H_{n\leftarrow \bullet}$
To others	$C^H_{\bullet\leftarrow 1}$	$C^H_{\bullet\leftarrow 2}$	$\dots$	$C^H_{\bullet\leftarrow 1}$	C^H

Note: Connectedness table as proposed by Diebold & Yilmaz (2014).

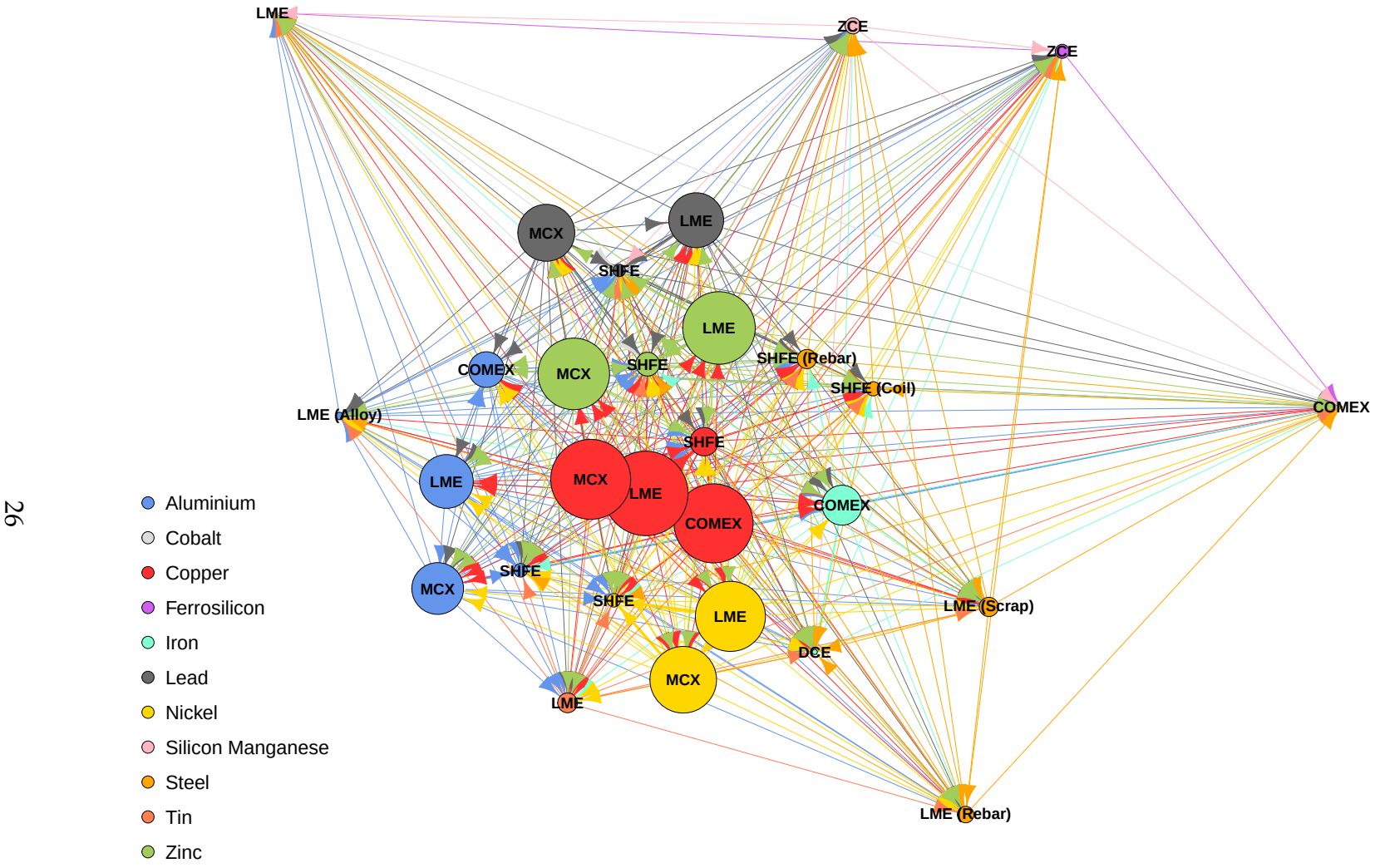

Figure 2: Network Representation of Return Spillovers

Note: Node size depends on total directional spillovers, arrow thickness and direction on net pairwise directional spillovers. Node placement is based on the graph drawing algorithm of Fruchterman & Reingold (1991).

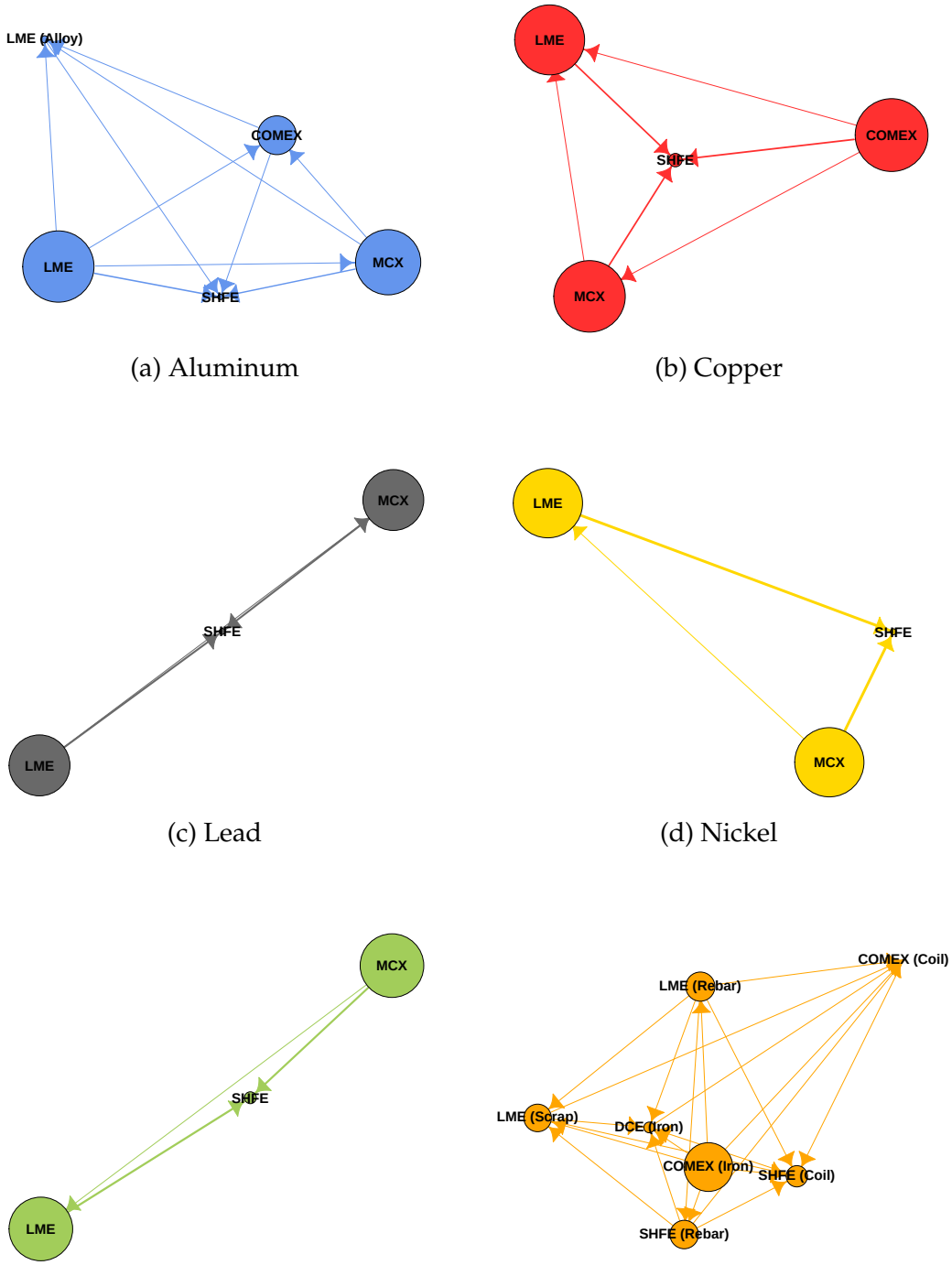

Figure 3: Individual Commodity Networks

Note: Node size depends on total directional spillovers, arrow thickness and direction on net pairwise directional spillovers. Node placement is based on the graph drawing algorithm of Fruchterman & Reingold (1991).

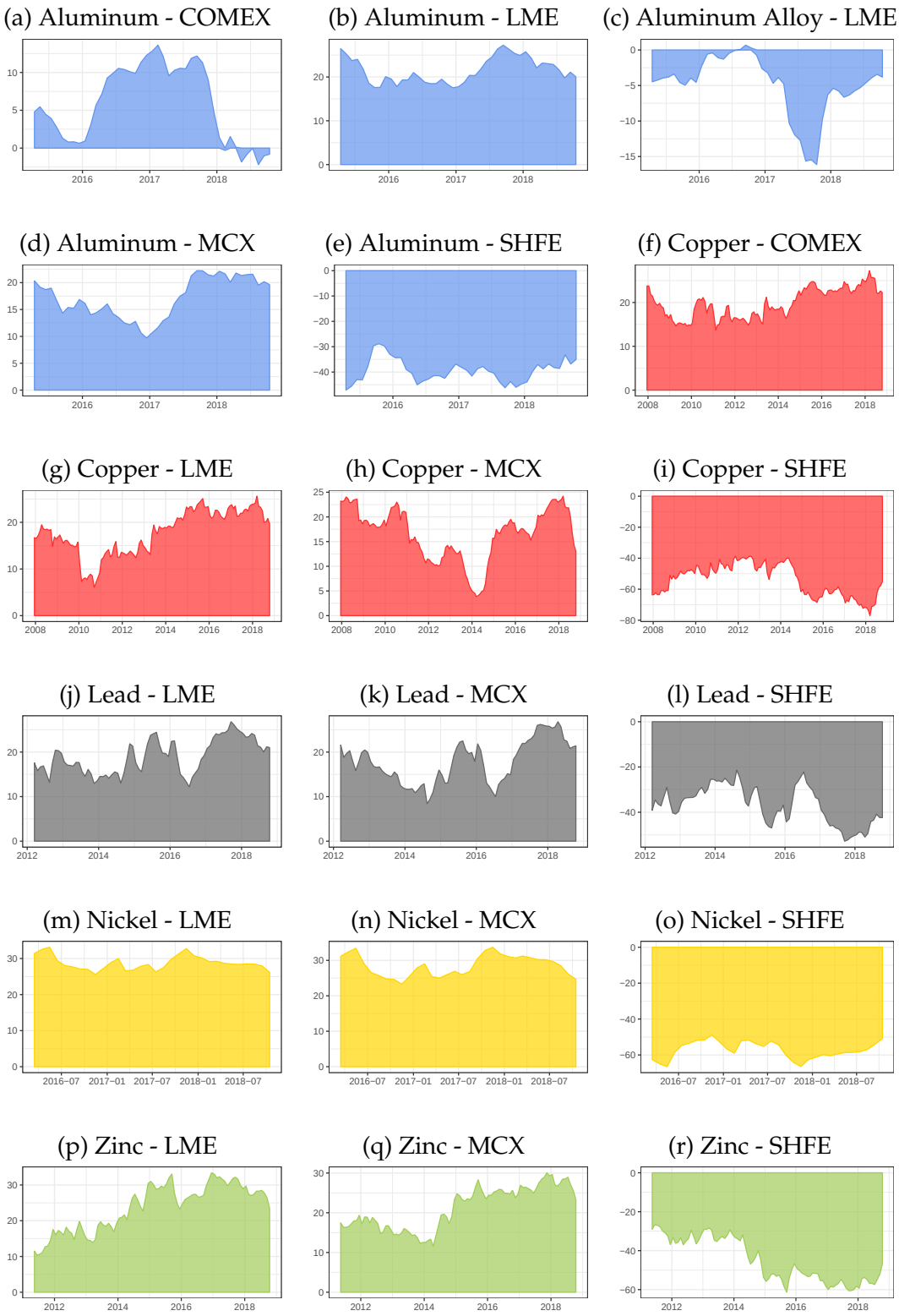

Figure 4: Time-Varying Net Spillovers

Note: The graphs show the time-varying net total directional spillovers of each futures contract. Values above zero indicate that a contract sends more price signals than it receives, whereas values below zero suggest the opposite.

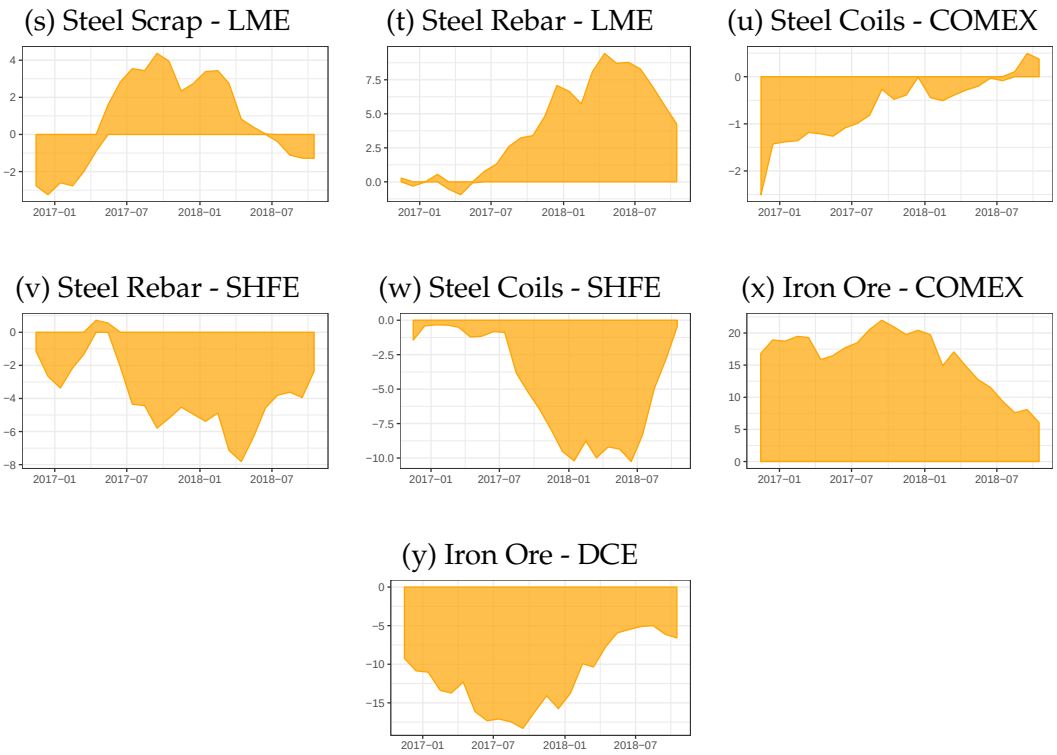

Figure 4 (cont.): Time-Varying Net Spillovers

Table 4: Regression Results

	Aluminum	Copper	Lead	Iron & Steel	Zinc
$C^{10}_{i\leftarrow j,t-1}$	1.044^{***}	0.947^{***}	0.922^{***}	0.923^{***}	0.929^{***}
	(0.027)	(0.011)	(0.013)	(0.013)	(0.013)
$VOLA_{j,t}$	0.007	-0.030^{***}	-0.023^{**}	0.012	-0.032^{*}
	(0.012)	(0.007)	(0.007)	(0.008)	(0.014)
$ILLIQ_{j,t}$	0.009	-1.076	-1.040^{***}	0.000	-8.847
	(0.006)	(0.685)	(0.122)	(0.000)	(7.750)
$SPMAT_{j,t}$	-0.000	0.000	-0.000	0.001^{*}	-0.000
	(0.000)	(0.000)	(0.000)	(0.000)	(0.000)
$IM_{ij,t}$	0.002	0.001	0.017	0.004	-0.229
	(0.007)	(0.001)	(0.085)	(0.007)	(1.204)
$EX_{ij,t}$	-0.012	0.001^{**}	0.021	0.002	0.017^{***}
	(0.012)	(0.000)	(0.018)	(0.002)	(0.003)
$TED_{j,t}$	0.060	0.021	-0.063	0.350^{*}	-0.079
	(0.191)	(0.033)	(0.074)	(0.185)	(0.053)
$VIX_{j,t}$	-0.004	-0.005	-0.034^{**}	-0.024	0.019^{**}
	(0.014)	(0.005)	(0.010)	(0.016)	(0.006)
$EPU_{j,t}$	0.000	0.000^{***}	0.000	0.001^{*}	0.000
	(0.000)	(0.000)	(0.000)	(0.000)	(0.000)
Const.	0.039	1.917^{***}	3.314^{***}	-0.673	2.987^{**}
	(0.658)	(0.452)	(0.528)	(0.451)	(0.923)
Overall R^2	0.993	0.997	0.995	0.962	0.994

Note: Standard errors in parentheses, $p < 0.1$, ** $p < 0.05$, *** $p < 0.01$